

Indirect Engine Sizing via Distributed Hybrid-Electric UAV State-of-charge Based Parametrisation Criteria

S. Wang[†], J.T. Economou^{††}, A. Tsourdost

[†]School of Aerospace, Transport, and
Manufacturing
Cranfield University
MK43 0AL, UK

^{††}Cranfield University
Cranfield Defence and Security,
Aeromechanical Systems Group
Centre for Defence Engineering
The Defence Academy of the United Kingdom
Shrivenham, SN6 8LA, UK.

^{††}Corresponding Author:
j.t.economou@cranfield.ac.uk

Abstract:

This paper presents a design process for the challenging problem of sizing the engine pack for a Distributed Series Hybrid Electric Propulsion System (DSHEPS) of Unmanned Aircraft Vehicle (UAV). Sizing the propulsion system for hybrid electric UAVs is a demanding problem because of the two different categories of propulsion, (the engine and the motor), and the electrical system characteristics. Furthermore, what adds to the difficulty is that the Internal Combustion Engine (ICE) does not directly drive the propellers, but it is connected to an electrical generator and therefore provides electrical power to the Electric Motors (EM) and propellers. Hence there is a clear distinction from the traditional engine solutions which are mechanically coupled to the propeller. This paper addresses this specific distinction and proposes an indirect solution based on properties on the electrical part of the system. In particular, a novel parametric characterisation engine sizing approach is presented using the battery pack State-of-Charge (SOC) during a realistic UAV flight scenario. Five candidate engine options were considered with different starting conditions for the electrical system. The results show that by using the SOC properties it is possible to select an appropriate size of engine pack while carrying a suitable electrical propulsion pack. However, the solutions are not unique and are appropriate for given design criteria clearly indicated in the paper.

Keywords: Hybrid UAV, Hybrid System Design, Series Hybrid, Distributed Hybrid system.

Introduction

In the past couple of decades, the largest growth in commercial air transport have a big impact and changed the world in numerous ways, primarily by increasing the speed of travel, aiding growth in the international business, and making the world more connected. However, a conventional aircraft consumes a large amount of fuel during each flight and simultaneously emits greenhouse gases, noise, heat, and particulates. To prevent the deterioration of aircraft negative impact on energy supply and

environment, a higher fuel-efficiency and more environmental-friendly propulsion system is required. In general, there are three ways to improve aircraft performance: (a) optimization of the existing aircraft propulsion systems; (b) development of new propulsion components, and (c) a combination of existing propulsion subsystems into hybrid powertrains. Based on the third method, this paper presents a novel Distributed Series Hybrid Electric Propulsion System (DSHEPS) for an UAV.

At present, NASA, Airbus, Boeing, and many other companies are investing in hybrid electric aircraft research to improve aviation performance. The most successfully-tested hybrid electric aircraft are UAVs and small-scale aircraft. Due to the fuel having higher power density than batteries', the fuel system contains more energy than an electric system for the same mass. Therefore, hybrid electric UAVs always can survive a longer flight. Hybrid UAVs emerged from 2010s, and to date, the one with the longest endurance is ALTI Transition, which offers up to 12 hours flight carrying no payload. University of Colorado Boulder [1], Queensland University of Technology [2], and U.S. Airforce Research Laboratory [3] all have researched this area. The other ongoing small hybrid aircraft project is AIRSTART, project in the UK, which is aiming to develop a parallel hybrid propulsion system to support routine small UAV operations beyond visual line of sight [4].

In terms of the hybrid electric midscale demonstrators, several aircraft have been successfully tested. Alatus motor-glider, designed by Cambridge University, firstly realized a parallel hybrid electric power system. It utilises a 2.8 kW internal combustion four-stroke leaf blower unit paralleled with a 12 kW electric motor, and the first truncated flight took place in 2010. Embry-Riddle Aeronautical University, in association with Google, designed another hybrid plane 'Eco-Eagle'. It also uses a parallel hybrid technology and was successfully tested in 2011 [5]. The first midscale series hybrid aircraft are the DA36 E-Star and its successor version, developed by Diamond Aircraft (DA), EADS, and Siemens AG in 2013 [6]. The series system of DA36 E-Star can provide 80 kW power during take-off and 65 kW continuous power during cruising. Later, Cambridge University developed another hybrid aircraft 'SOUL', which firstly realized the capability of on-board battery charging. It applies a parallel hybrid electric propulsion system and was successfully tested in 2014 [7].

Research in large-scale aircraft has increased over the recent years. The new series of aircraft from NASA are particularly designed using hybrid electric propulsion systems. For example, the N3-X Hybrid Wing Body Turboelectric Plane [8] and the STARC-ABL Turboelectric Plane [9] utilise gas-turbine/electric hybrid propulsion systems; the SCEPTOR X-57 plane uses an engine/electric hybrid power system [10]; and the Subsonic Ultra Green Aircraft applies a liquefied natural gas fuel cell/electric hybrid propulsion system [11]. Meanwhile, Airbus, Rolls-Royce, and Siemens are working together to test the feasibility of a hybrid electric propulsion system in a relatively large aircraft, called E-Fan X Plane, and the test flight is currently planned in 2020 [12].

As hybrid electric aircraft are becoming increasingly more popular, new attempts to develop different hybrid aircraft are expected to increase. Therefore, the method for reasonable designing and sizing of Hybrid Electric Propulsion System (HEPS) is also essential. Many optimal sizing works have been conducted in the literature. Most studies focus on single objective optimization, e.g. the paper [13] optimized the capacity of different components of a hybrid system using the loss of power supply probability and the 'Levelised' cost of energy. A small number of studies focuses on multi-objective optimization, which is able to optimize both system performance and other criteria [7] [14]. The paper [15] presents a method to optimize plant parameters and minimize the total fuel consumption simultaneously. However, none of the previous research discussed the relationship of battery's performance and parameter sizing. In this paper, we present a novel parametric engine sizing approach to size the engine pack for a hybrid electric UAV. From simulation results, i.e. batteries pack SOC, the characteristics of five systems with different sized engines are obtained and analysed.

Therefore, based on a set flight scenario, a reasonable engine size region can be determined. The proposed design sizing approach provides a new cognition of series hybrid electric systems, especially focusing towards the relationship and synergy between fuel and electricity.

DSHEPS Design Process

Within a simplified system design progress, as shown in Figure 1, the DSHEPS is designed. The system is basically derived from a conventional series HEPS configuration, integrated with the Distributed Propulsion (DP) concept and the More Electric Aircraft (MEA) concept, the resulting system has improved fuel economics and emits fewer emissions.

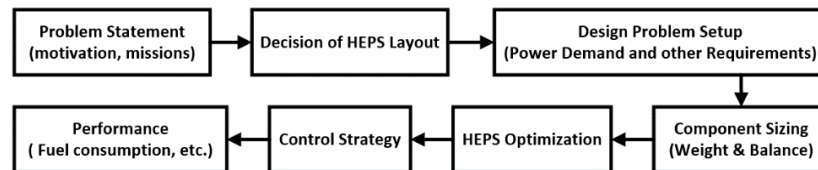


Figure 1 System design sequence.

In general, hybrid systems are categorized into series, parallel and complex hybrid. In particular, the series hybrid system has similar properties to a pure electric system, thus resulting in emission reduction. Furthermore, an additional important advantage of the series configuration is the decoupling between demand and supply. Engines can continuously operate at the most optimal operating point regardless of power requirement, which provides an enormous improvement on fuel efficiency. In addition, due to the high degree of electrification, mechanical linkages are not necessary so that all system components can be positioned at different locations within the UAV which increases subsystem level flexibility as shown in Figure 2.

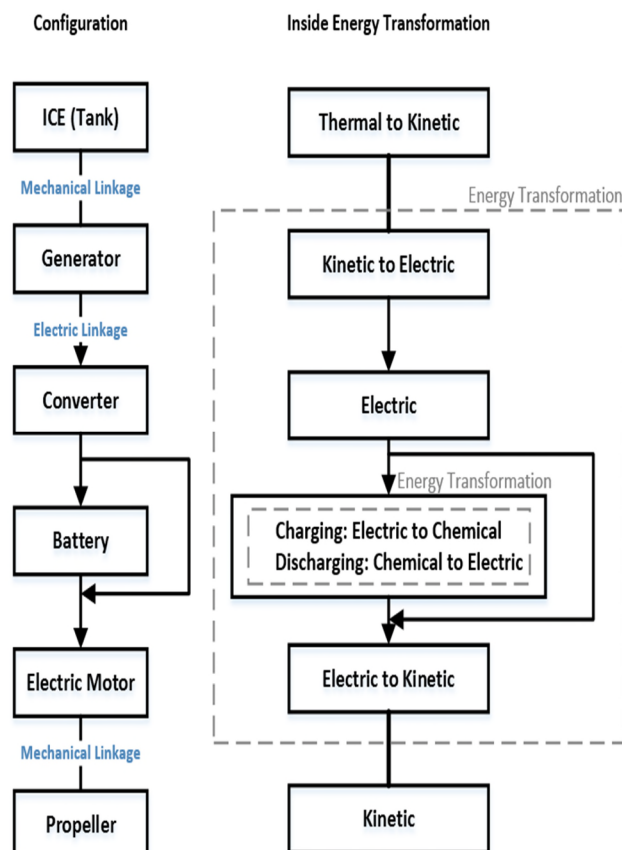


Figure 2 Series propulsion system configuration and internal energy transformation.

However, series HEPSs have two persistent drawbacks: over-weight and inevitable energy loss. Normally this is because of the extra generator, battery and large EM. Increasing the overall aircraft weight will consequently cost more fuel to complete the same mission. This is a challenge which needs solving. The other drawback is the energy conversion loss due to the multiple energy transformations, i.e. kinetic energy to electrical energy, electrical energy to chemical energy. Although the engine can operate at the high-efficiency area, it cannot be guaranteed that the series hybrid systems will have an increased efficiency. Therefore, in order to resolve these challenges, the DP concept and the MEA concept are integrated.

The designed complete DSHEPS is shown in Figure 3 and Figure 4. For easier analysis, we divided the system into three parts: power source, propulsion load and other loads. The 'power source' consists of an engine, a generator, a converter, and batteries. All devices provide electricity to the loads or/and stores electricity in the batteries. The second part 'propulsion load' includes converters, motors, and propellers. Motors are arranged symmetrically and connected to a corresponding propeller. Here, converters are not necessary if the rated voltage of motors are same as it of the main electric net (in this paper, the simulation neglects converters). The 'other loads' represents the auxiliary electric loads including an electric taxiing system, avionics systems etc.

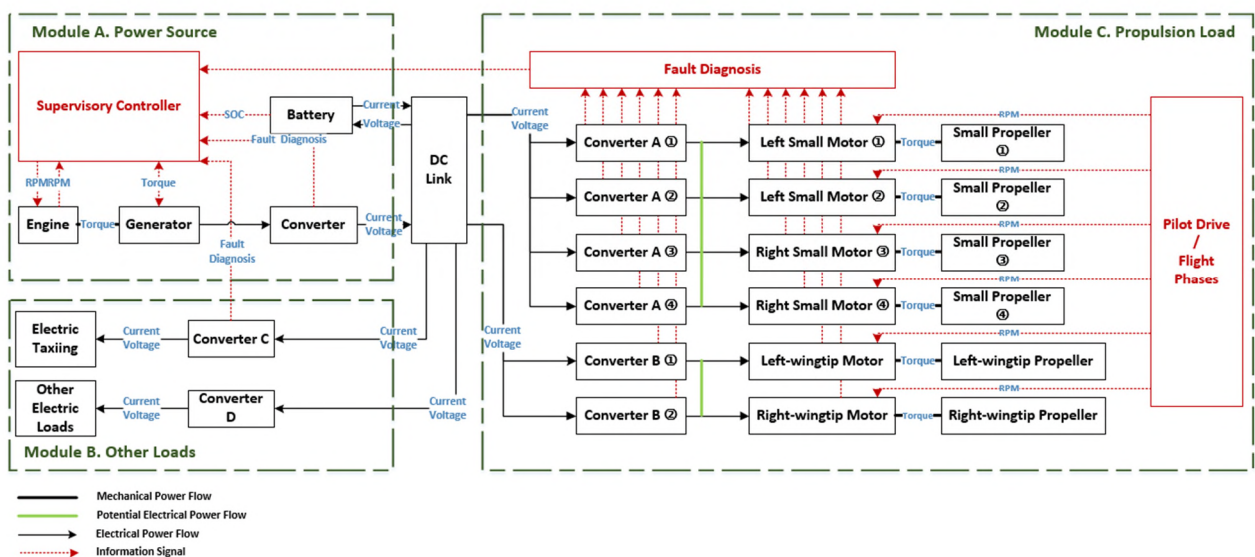


Figure 3 The complete distributed series hybrid electric propulsion system.

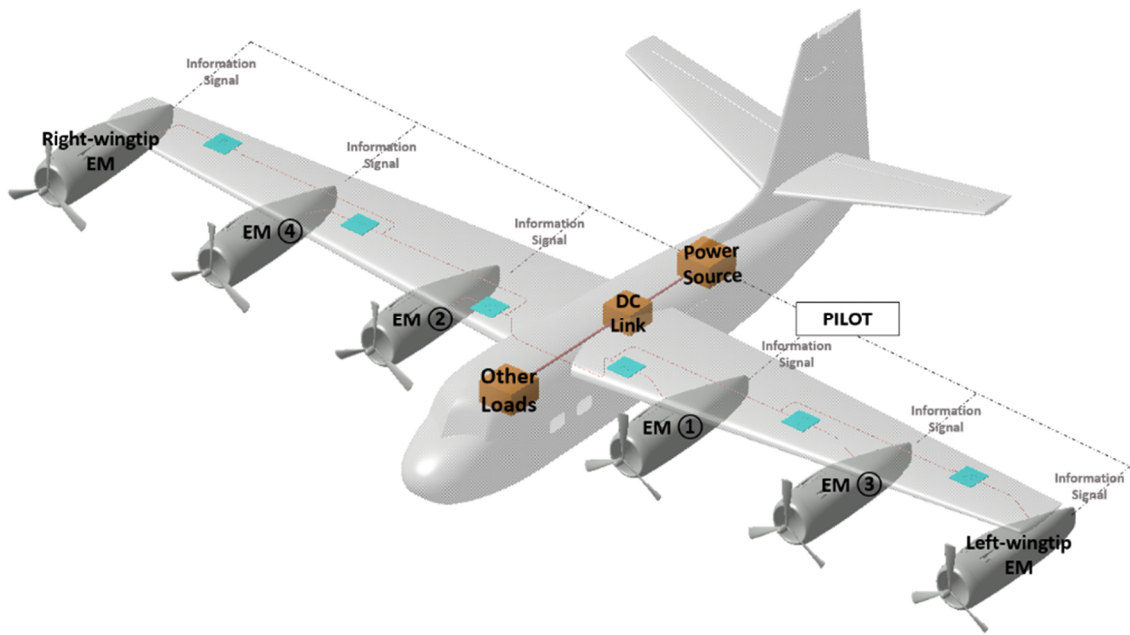


Figure 4 The complete distributed series hybrid propulsion system layout.

According to the ‘propulsion load’ block shown in Figure 3, the designed system has six small motors instead of using a single motor. Applying multi small electric propulsion has many benefits. Firstly, it provides a robust propulsive control and enhances flight safety when an EM might stop operating safely. Moreover, as engines are normally sized as large as twice the power demand for redundancy reasons. For example, a Boeing 737, 757, 767 and 777 can take off with one of two engines out. The DP architecture reduces the excess weight from the extra engine since one extra small motor provides equal flight safety as one extra big engine in conventional aircraft. Additionally, DP concept increases the dynamic pressure over the wing and reduces aerodynamic drag [16] [17] [18] [19], so that it can reduce the wing area, lighten the aircraft structure, and reduce power demand.

Similarly, inspired by the MEA concept [20] [21] [22], some improvements are made into the system. The most important improvement is the expanded electric network. Here, the engine not only provides propulsion power but also transports electric energy to all existing electric loads (flight control actuation, fuel pumping, etc.). This integration removes unnecessary electronic equipment, reduces system weight, eases the maintenance and improves system efficiency. The second improvement is the adoption of the electric taxiing concept. The electric taxiing system is more efficient and safe. Also, the engine can be turned off earlier, which can reduce engine’s operating time and reduce fuel consumption.

SOC Based Criteria for Aircraft Engine Sizing

As the system isolates the engine from the demand, the engine sizing becomes less challenging. To reassure safety, there are three requirements in this paper:

The engine can continuously generate power on a low fuel consumption rate.

Batteries can fill the gap between total power requirement and engine output.

Motors can provide enough torque and speed to propellers.

Table 1 Example UAV parameters.

| | | | |
|----------------------------|--------|---------------------|-----------------------|
| Drag coefficient, C_D | 0.067 | Wing area, A | 3.76 m ² |
| Lift coefficient, C_L | 0.614 | Air density, ρ | 1.1 kg/m ³ |
| Indicated airspeed, v | 50 m/s | Lift to drag ratio | 9.16 |
| Maximum take-off mass, m | 150 kg | Cruising altitude | 1000 m |

The properties of the example UAV are shown in Table 1 [23]. Based on this information, the power demand for cruising could be determined by the following equations. The aerodynamic drag D is depended on the drag coefficient C_D , the surface area over the air flows A , the density of the air ρ , and the square of the velocity v^2 . Because the cruising altitude is approximately 1000m, the required power for cruising is about $P = 17 \text{ kW}$. Assuming the motor efficiency is 98% and the batteries efficiency is 99%, the required power for engine P_{req} could be determined.

$$D = \frac{1}{2} C_D A \rho v^2 \quad (N) \quad (1)$$

$$P = Dv = \frac{1}{2} C_D A \rho v^3 \quad (N) \quad (2)$$

$$P_{req} = \frac{17 \text{ Kw}}{98\% * 98\% * 99\%} \approx 18 \text{ kW} \quad (3)$$

Therefore, the flight scenario and the engine power requirement are both determined, as shown in Figure 5. Please note that the assumption of a constant thrust level leads to slight inaccuracies in the determination of the required energy.

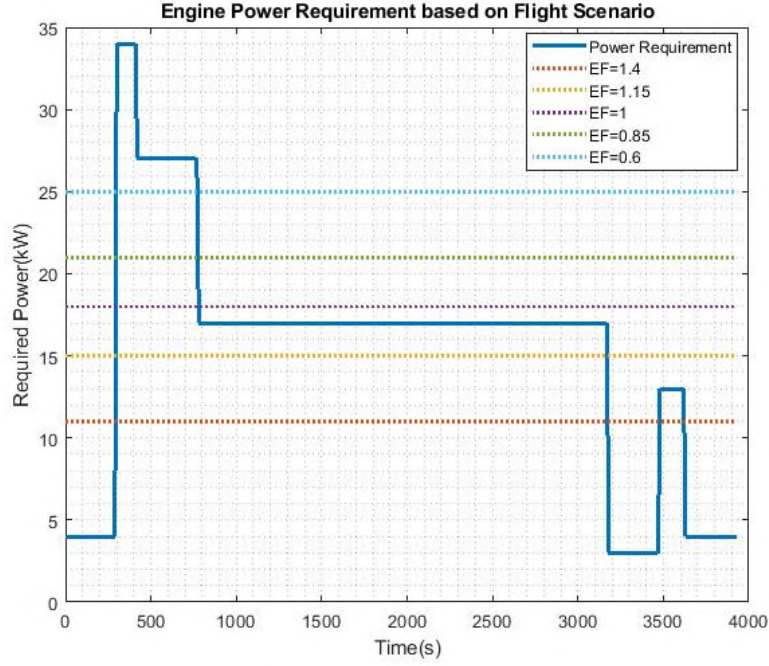


Figure 5 The power requirement of flight scenario and the ideal power of each engine.

To find an appropriate engine and observe the parametric variation, several engines have been simulated. These engines are selected based on a hybridization factor. The hybridization factor is a parameter mirroring the relationship between the sizes of the different power sources [24]. The first hybridization factor HF was introduced by Lukic and Emadi [25]:

$$HF = \frac{(P_{EM_max} - P_{E_max})}{P_{EM_max}} \quad (4)$$

P_{EM_max} and P_{E_max} are the maximum power of motor and engine. The original hybridization factor HF shows the importance of the engine or the motor as part of the whole system. However, since the engine is always operating at its most efficient point, HF is difficult to clearly describe the proportion of electric energy and kinetic energy. Therefore, two other factors HF_{opt} and EF are developed for this paper, as shown in Equation (5) and (6). P_{E_opt} is the engine output power at the most efficient area, and P_{req_av} is the average power of the mission requirement. Engines are selected from $0.6EF$ to $1.4EF$, and the detailed information is represented in Table 1.

$$HF_{opt} = \frac{(P_{EM_max} - P_{E_opt})}{P_{EM_max}} \quad (5)$$

$$EF = \frac{P_{E_opt}}{P_{req_av}} \quad (6)$$

Table 2 Specifications of engines, motors, and batteries.

| Engine type | Max continuous power | Lowest-fuel-rate power | HF_{opt} | EF |
|-----------------|----------------------|------------------------|--------------|------|
| RT300LCR | 20kW @6500RPM | 11kW @5000RPM | 0.89 | 0.60 |
| RT300XE | 21kW @6500RPM | 15kW @5250RPM | 0.85 | 0.85 |
| RT600JET-A1 | 38kW @6500RPM | 19kW @4500RPM | 0.81 | 1.00 |
| RT600LCR | 40kW @6500RPM | 21kW @4750RPM | 0.79 | 1.15 |
| RT600XE | 52kW @6500RPM | 25kW @4750RPM | 0.75 | 1.40 |
| Motor type | Max continuous power | Max power | Efficiencies | |
| EMRAX228 | 42kW | 100kW | 96% | |
| Batteries | Capacity | Nominal voltage | Efficiencies | |
| Li-Po batteries | 13Ah | 296V | 98% | |

Simulation Results and Discussion

A key part of the design process is to explore the parametric variations prior to building a prototype UAV, thus reducing the design and development costs. Therefore, three simulations are processed for each selected engine with different initial SOC: $SOC_A(t=0) = 50\%$, $SOC_B(t=0) = 75\%$ and $SOC_C(t=0) = 100\%$. Engines has three fundamental operating modes: (a) the electric mode, (b) the ideal mode, and (c) the maximum power mode. Mode conversions are triggered by the SOC. In this paper, the high threshold is set as 80% and the low threshold is set at 20%. Namely, when the SOC is beyond 80%, the system will switch into the electric mode; while if the SOC is below 20%, the system will switch into the maximum power mode. Moreover, this system incorporates a gap which results in obtaining an extra 10% SOC during the charging process. If the batteries were in the charging mode, the system will be switched back to the ideal mode at 90% SOC instead of 80%. This setting has dual purposes, which not only guarantees the power output, but also protects batteries.

Figure 6 shows the SOC curve of each simulation. When simulations start with a full SOC_C , all simulations began from the electrical mode. Gradually, when the SOC drops below 80%, the differences of various engines began to show up by the altered discharging rate. Amongst them, RT600XE is the most powerful engine and firstly recharged back to 80% SOC. Since its ideal power output is about 1.4 times of the average power demand, the SOC stays in 80%-90% area for most of the flight. RT600LCR engine recovers to 80% SOC as well but at a slower rate than RT600XE. RT600JET outputs just the right power as demanded at its ideal operating point. The SOC stays stable during the cruise mode. RT300XE and RT300LCR cannot provide enough power even for the average power demand for the specific UAV parameters. Their SOC dropped below 20% and jumped to maximum power mode. The fuel consumption rate during the maximum power mode is not as good as the ideal mode, but they are powerful to generate electricity and guaranteed that batteries are not fully depleted.

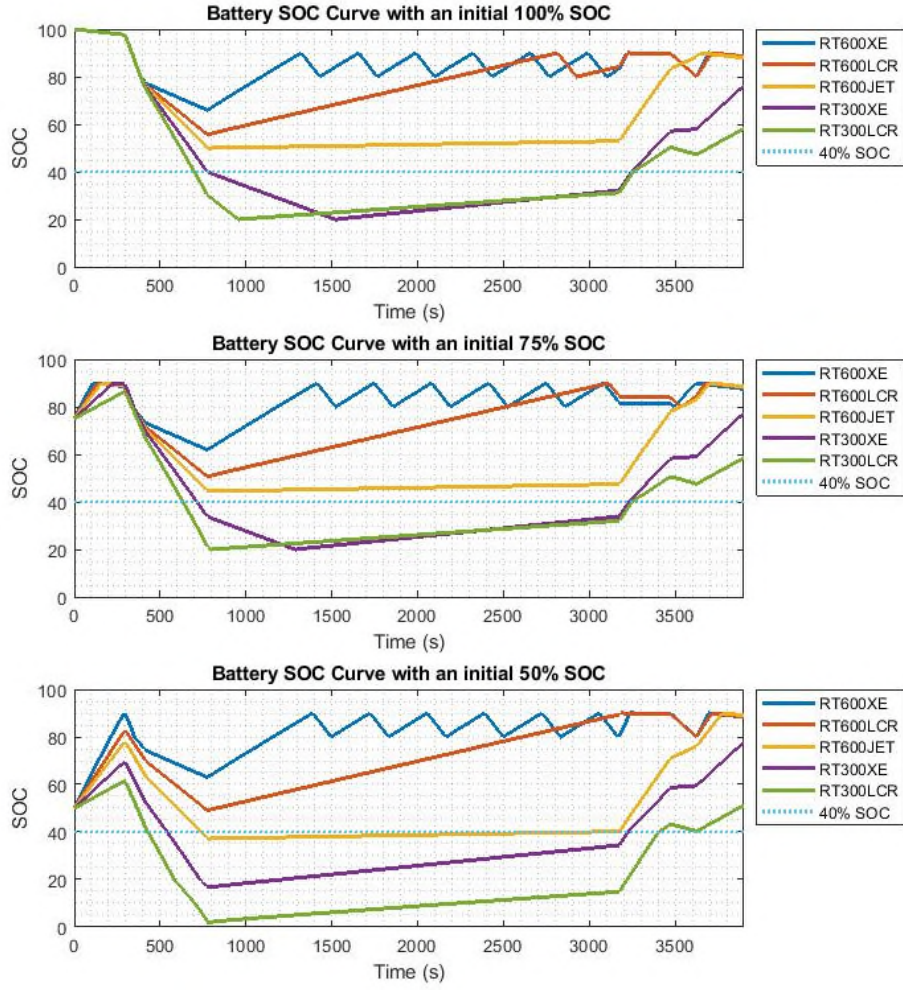


Figure 6 Batteries SOC curves.

With an initial 75% SOC_B and 50% SOC_A , small engines can easily drop below 20% and trigger the maximum power operating mode. The SOC for RT300LCR was nearly 0 in its third simulation, which shows that although it was in maximum power mode, it cannot stop SOC decrease during a high-powerful requirement. In addition, it can be seen that RT600JET, RT600LCR and RT600XE have three similar SOC curve. For these three engines, no matter how much is the initial SOC, batteries have a similar performance. An alternative hybridization factor $HF_{realtime}$ is introduced to estimate the ratio of power which comes which relates to batteries power P_B and motor output P_{EM} .

$$HF_{realtime} = 1 - \frac{P_B}{P_{EM}} \quad (7)$$

While the system is running, the $HF_{realtime}$ is calculated to show the “degree of electrification” and the importance of electricity by second. These results are summarized in Figure 7 and

Table 3.

Table 3 Simulation results.

| | | 50% SOCA (t=0) | 75% SOCB (t=0) | 100% SOCC (t=0) |
|----------|-------------------------|-------------------|-------------------|--------------------|
| RT600XE | Electric Mode | 1305 s | 1462 s | 1648 s |
| | Ideal Mode | 2595 s | 2438 s | 2252 s |
| | Max Power Mode | 0 | 0 | 0 |
| | Average $HF_{realtime}$ | 73% | 77% | 69% |
| RT600LCR | Electric Mode | 631 s | 851 s | 1081 s |
| | Ideal Mode | 3269 s | 3049 s | 2819 s |
| | Max Power Mode | 0 | 0 | 0 |
| | Average $HF_{realtime}$ | 85% | 84% | 77% |
| RT600JET | Electric Mode | 124 s | 382 s | 642 s |
| | Ideal Mode | 3776 s | 3518 s | 3258 s |
| | Max Power Mode | 0 | 0 | 0 |
| | Average $HF_{realtime}$ | 85% | 84% | 80% |
| RT300XE | Electric Mode | 0 | 116 s | 386 s |
| | Ideal Mode | 1407 s | 1840 s | 1789 s |
| | Max Power Mode | 2493 s | 1944 s | 1725 s |
| | Average $HF_{realtime}$ | 84% | 80% | 77% |
| RT300LCR | Electric Mode | 0 | 0 | 386 s |
| | Ideal Mode | 1078 s | 1449 s | 1215 s |
| | Max Power Mode | 2822 s | 2451 s | 2299 s |
| | Average $HF_{realtime}$ | 80% | 77% | 73% |

From these results, it can be seen that RT 600JET is operating at ideal conditions and its final SOC is the same as RT600LCR and RT600XE. RT600JET avoids the frequent mode conversions and can achieve a high SOC at the end of the mission. Therefore, if the vehicle is not specially designed for an electric mode, it is not necessary to have a big engine.

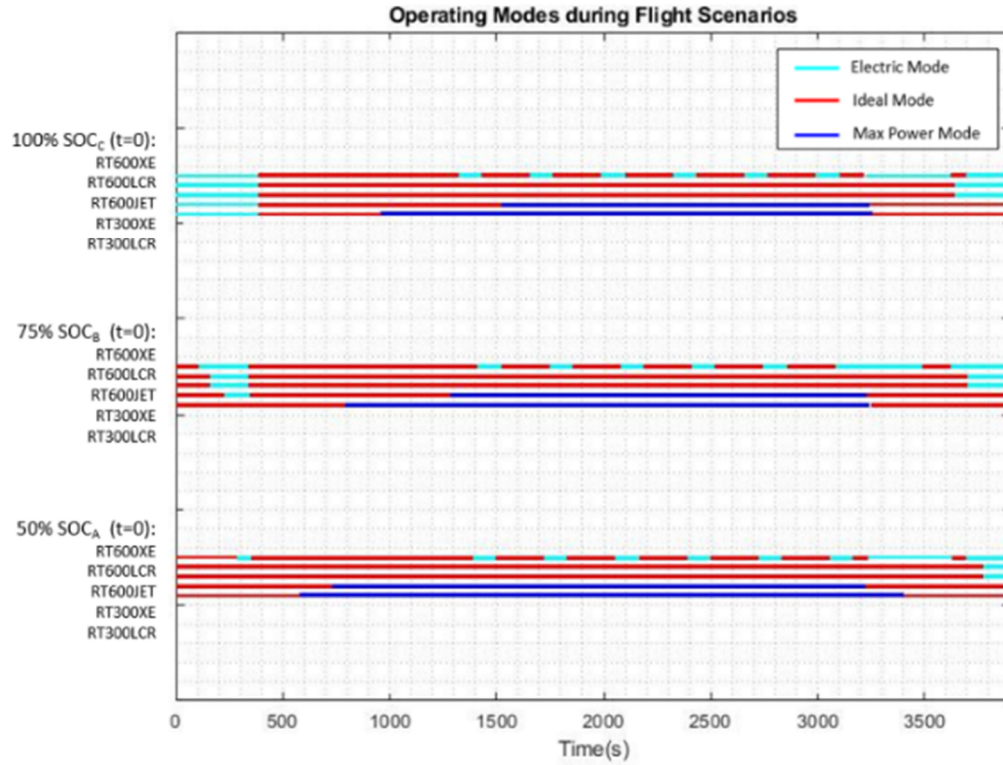


Figure 7 Operating modes during flight scenario.

Figure 8 illustrates the length of time remaining under 40% SOC during each simulation. From this figure, it can be observed that SOC of RT600XE and RT600LCR have not been to a value under 40%. The SOC of RT600JET was once under 40% SOC when $SOC_A(t = 0) = 50\%$. But from Figure 6, it can be determined that the SOC is around 40% and the lowest SOC value is about 38%. It has not dropped to the low boundary of 20% SOC. For the other two small engines, although the initial SOC is different, the length of time remaining under 40% SOC is similar. Because SOC_B and SOC_C tests have a charging procession at the beginning of the flight, they performed similarly. However, due to the difference of the result of SOC_A and SOC_B is small, it can be deduced that the initial SOC has less influence for a system operating, engine size indeed influences the system performance. The HEPS requires an engine which can provide equal amount of energy of the average value of power demand at its lowest fuel consumption rate point.

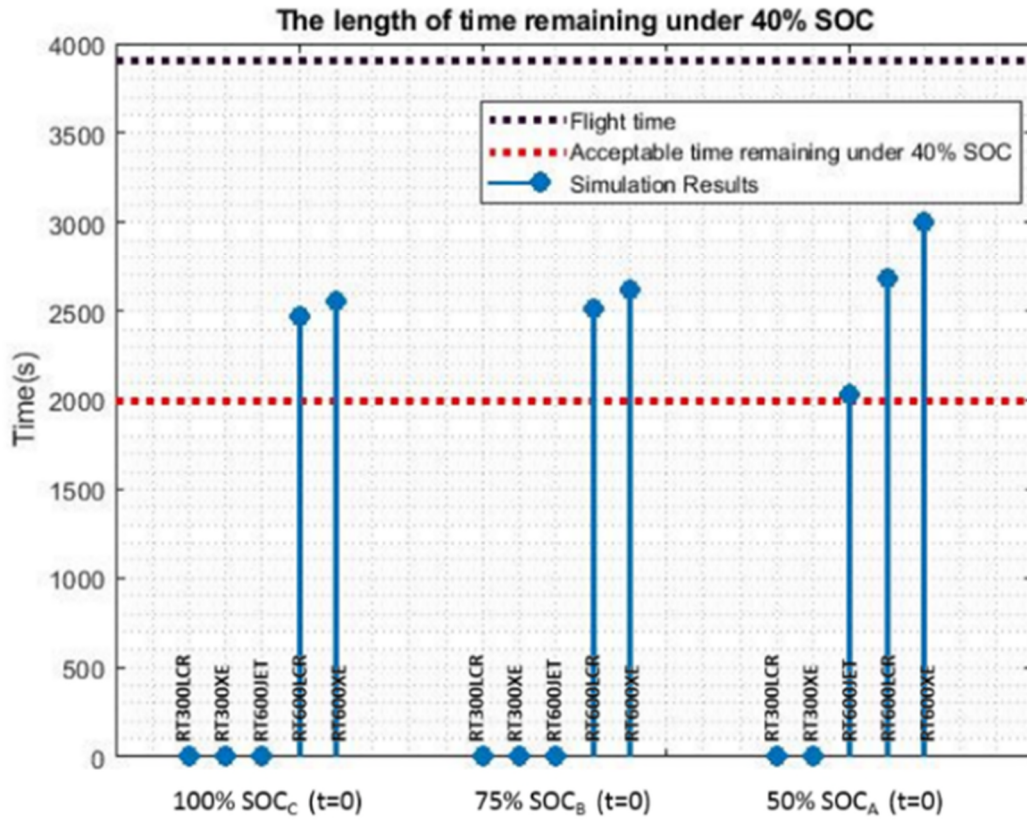


Figure 8 The length of time remaining under 40% SOC.

Conclusions

The UAV simulations were repeated for three cases: SOC_A , SOC_B , SOC_C with initial battery pack state-of-charge $SOC_A(t=0) = 50\%$, $SOC_B(t=0) = 75\%$ and $SOC_C(t=0) = 100\%$ respectively for the defined UAV mission flying scenario. For each one of the three state-of-charge five combustion power sizes (RT600XE, RT600LCR, RT600JET, RT300LCR, RT300XE) were simulated to explore if the SOC will enter the range of less than 40% which is considered the acceptance criterion.

From all the results presented the five different power pack options performed well however two did not meet the minimum SOC criterion: RT300LCR and RT300XE. Clearly using the proposed approach the design team can select for different flight scenarios and range of engine packs (five in this case) the best option for a range of initial pre-flight battery pack SOC. The design sizing approach is effective because it links the combustion engine power pack operation and choice of size with the battery pack and also the power pack initial conditions.

The next step of research is to optimize the entire propulsion system design by using genetic algorithms. Each subsystem would be selected according to the total system weight and the estimated fuel consumption. Furthermore, a trade-off study of fuel efficiency and emissions will be conducted, and an intelligent controller with configurability will also be designed.

Table of Symbols

| | | |
|-----------------|--|----------|
| A | Wing area | m^2 |
| C_D | Drag coefficient | — |
| C_L | Lift coefficient | — |
| D | Aerodynamic drag | N |
| EF | Engine factor | — |
| m | Maximum take-off weight | kg |
| ρ | Air density | kg/m^3 |
| P | Power | W |
| P_{req} | Required power | W |
| P_{EM_max} | Maximum power of the motor | W |
| P_{E_max} | Maximum power of the engine | W |
| P_{E_opt} | Engine power at its most efficient point | W |
| P_{req_av} | Average value of power requirement | W |
| P_B | Battery output power | W |
| P_{EM} | Motor output power | W |
| HF | Hybridization factor | — |
| HF_{opt} | HF using P_{E_opt} | — |
| $HF_{realtime}$ | Real-time hybridization factor | — |
| SOC | State of charge | — |
| v | Aircraft airspeed | m/s |

References

- 1 Koster J, Velazco A and Munz C, Hyperion UAV: An International Collaboration, 50th AIAA Aerospace Sciences Meeting including the New Horizons Forum and Aerospace Exposition, Aerospace Sciences Meetings, Nashville, 2012 Jan.
- 2 Glasscock R, Hung J and Gonzalez L, Multimodal Hybrid Powerplant for Unmanned Aerial Systems (UAS) Robotics, Twenty-Fourth Bristol International Unmanned Air Vehicle Systems Conference, Bristol, United Kingdom, 2009 Mar.
- 3 Ausserer J and Harmon F, Integration Validation and Testing of a Hybrid-Electric Propulsion System for a Small Remotely Piloted Aircraft, 10th International Energy Conversion Engineering Conference, Georgia, 2012.
- 4 Xie Y, Savvaris A and Tsourdos A, Modelling and control of a hybrid electric propulsion system for unmanned aerial vehicles, 2018 IEEE Aerospace Conference, Big Sky, MT, 2018.
- 5 Talbert T, The EcoEagle, National Aeronautics and Space Administration, 2012 Aug.
- 6 Siemens, Diamond Aircraft and EADS, World's first serial hybrid electric aircraft to fly at Le Bourget, Siemens, Diamond Aircraft and EADS, Munich, 2011.
- 7 Friedrich C and Robertson P.A, Hybrid-Electric Propulsion for Aircraft, Journal of Aircraft, 2015; 52: 176-189.
- 8 National Aeronautics and Space Administration, Overview of Subsonic Fixed Wing Project: Technical Challenges for Energy Efficient, Environmentally Compatible Subsonic Transport Aircraft, 3rd NASA Glenn Propulsion Control & Diagnostics Workshop, Cleveland OH, 2012.
- 9 Welstead J and Felder J.L, Conceptual Design of a Single-Aisle Turboelectric Commercial Transport with Fuselage Boundary Layer Ingestion, 54th AIAA Aerospace Sciences Meeting, AIAA SciTech Forum, California, USA, 2016.
- 10 Moore M.D, Distributed Electric Propulsion (DEP) Aircraft, National Aeronautics and Space Administration, 2014.
- 11 Bradley M.K and Droney C.K, Subsonic Ultra Green Aircraft Research Phase II: N+4 Advanced Concept Development, National Aeronautics and Space Administration, California, 2012.
- 12 Siemens, Airbus and Rolls-Royce, Airbus, Rolls-Royce, and Siemens team up for electric future, London, 2017.
- 13 Yang H, Lu L and Zhou W, A novel optimization sizing model for hybrid solar-wind power generation system, Solar Energy, 2007; 81: 76-84.
- 14 Seeling-hochmuth G.C, A combined optimisation concept for the design and operation strategy of hybrid-PV energy system, solar energy, 1997; 61(2): 77-87.
- 15 Zou Y, Sun F and Hu X, Combined Optimal Sizing and Control for a Hybrid Tracked Vehicle, Energies, 2012; 5: 4697-4710.
- 16 Deere K.A, Viken J.K and Viken S, Computational Analysis of a Wing Designed for the X-57 Distributed Electric Propulsion Aircraft, 35th AIAA Applied Aerodynamics Conference, AIAA AVIATION Forum, 2017.
- 17 Stoll A.M, Bevirt J and Moore M.D, Drag Reduction Through Distributed Electric Propulsion, 14th AIAA Aviation Technology, Integration, and Operations Conference, AIAA AVIATION Forum, 2014.
- 18 Papathakis K.V, NASA Armstrong Flight Research Center Distributed Electric Propulsion Portfolio, Safety and Certification Considerations, 2017.
- 19 Brelje B.J, Martins J.R.R.A, Development of a Conceptual Design Model for Aircraft Electric Propulsion with Efficient Gradients, Electric Aircraft Technologies Symposium (EATS) 2018 AIAA/IEEE, 2018.
- 20 Wheeler P.W, Clare J.C., Trentin A and Bozhko S, An overview of the more electrical aircraft. Proceedings of the Institution of Mechanical Engineers, Part G: Journal of Aerospace Engineering, 2013; 227: 578–585.

- 21 Naayagi R.T, A review of more electric aircraft technology, 2013 International Conference on Energy Efficient Technologies for Sustainability, Nagercoil, India, 2013.
- 22 Hafez A.A.A, Forsyth A, A Review of More-Electric Aircraft, 13th International Conference on Aerospace Sciences and Aviation Technology, 2009.
- 23 Dunne A, Aerodynamic Analysis and Optimization of the Aegis UAV, MSc Thesis, Cranfield, the United Kingdom, 2012.
- 24 Friedrich C and Robertson P.A, Design of Hybrid-Electric Propulsion Systems for Light Aircraft, 14th AIAA Aviation Technology, Integration, and Operations Conference, AIAA Aviation Forum, 2004.
- 25 Lukic S.M and Emadi A, Effects of drivetrain hybridization on fuel economy and dynamic performance of parallel hybrid electric vehicles, in IEEE Transactions on Vehicular Technology, 2004 Mar; 53(2): 385-389.

Indirect engine sizing via distributed hybrid-electric unmanned aerial vehicle state-of-charge-based parametrisation criteria

Wang, Siqi

2019-04-28

Attribution-NonCommercial 4.0 International

Wang S, Economou JT, Tsourdos A. (2019) Indirect engine sizing via distributed hybrid-electric unmanned aerial vehicle state-of-charge-based parametrisation criteria. Proceedings of the Institution of Mechanical Engineers, Part G: Journal of Aerospace Engineering, Volume 233, Issue 14, 2019, pp. 5360-5368

<https://doi.org/10.1177/0954410019843722>

Downloaded from CERES Research Repository, Cranfield University